NASA TN D-621

Copy 1

EXTRA COPY

TECHNICAL NOTE

D-621

EXPERIMENTAL AND CALCULATED FLOW FIELDS PRODUCED BY AIRPLANES FLYING AT SUPERSONIC SPEEDS

By Harriet J. Smith

Flight Research Center
Edwards, Calif.

NATIONAL AERONAUTICS AND SPACE ADMINISTRATION
WASHINGTON
November 1960

NATIONAL AERONAUTICS AND SPACE ADMINISTRATION

TECHNICAL NOTE D-621

EXPERIMENTAL AND CALCULATED FLOW FIELDS PRODUCED BY AIRPLANES FLYING AT SUPERSONIC SPEEDS

By Harriet J. Smith

SUMMARY

Results are presented of a flight investigation conducted to survey the flow field generated by airplanes flying at supersonic speeds. The pressure signatures of an F-100, an F-104, and a B-58 airplane, representing widely varying configurations, at distances from 120 to 425 feet from the generating aircraft and at Mach numbers from 1.2 to 1.8 are shown.

Calculations were made by using Whitham's method and were compared with the experimental results. The procedure used for calculating Whitham's $F(y)$ function is given in the appendix. Good agreement was obtained for the bow shock-wave strength, and overall characteristics of the flow field were predicted; however, all details of the flow field were not accurately predicted. This was especially true at the higher Mach numbers. Since the area distribution used in the calculations was for a Mach 1 equivalent body of revolution, experiments were made to obtain the Mach line area distribution for one of the configurations. When this area distribution was used in the calculations, the results were improved.

INTRODUCTION

The flow field generated by an airplane flying at supersonic speeds can be separated into three regions: local, far, and near fields. The local flow field extends from the body surface to approximately the wing tips. The flow in this region is important in determining the interference effects of one airplane component on another component. The far field is that region where all the intermediate shocks have joined and only the bow shock and rear shock remain. This flow field is especially important in estimating the noise on the ground produced by supersonic airplanes flying at high altitudes. The near field is the region beyond the wing tips of the airplane and including the intermediate shocks produced by the canopy and wings. Determination of the flow pattern in this area is necessary in assessing the danger involved in close-formation

flying, aerial-refueling operations, and other situations involving close approaches or passes. In reference 1 it was shown that, at supersonic speeds, appreciable motions can be induced on an airplane flying in proximity to another airplane. In addition, when an airplane is flown at supersonic speeds at extremely low altitudes, it is necessary to take into account the entire shock pattern to predict ground pressures and damage to ground establishments.

Much theoretical work has been done to predict these flow fields. The method of characteristics (ref. 2) has been used with considerable success in predicting local-flow characteristics. The method developed by Whitham (ref. 3) is applicable to both the near field and the far field. This method has been used previously (refs. 4 to 6) to predict the far field and has been shown to give excellent agreement with experimental data.

This paper is concerned with the flow in the near field and presents both experimental and theoretical data. Three airplanes (fig. 1), an F-100, an F-104, and a B-58, were used in these tests to obtain the experimental flight data. Pressure measurements were made at several distances from each airplane to determine the effects of body shape and distance away from the airplane on the shape and intensity of the shock pattern. In addition, Whitham's method was used to determine if these results could be accurately predicted.

SYMBOLS

$$F(y) = \frac{1}{2\pi} \int_0^y \frac{S''(t)dt}{\sqrt{y - t}}$$

i,m,n integers

$k = 2^{-1/2}(\gamma + 1)M^4\beta^{-3/2}$

l length of airplane

l_{ff} length of flow field

M Mach number

p_0 static pressure, lb/sq ft

Δp incremental pressure, lb/sq ft

S	cross-sectional area
t	variable
x	longitudinal coordinate
y,r	cylindrical coordinates (y, measured along body axis; r, radial coordinate perpendicular to y)
$\beta = \sqrt{M^2 - 1}$	
γ	ratio of specific heats for air (1.4)

A prime (') is used to denote the first derivative of a function; a double prime (") denotes second derivatives.

DESCRIPTION OF TESTS

The flight-test procedure used in this investigation to obtain the experimental data on supersonic flow fields is illustrated in figure 2.

The flow field to be measured was generated by the lead airplane, which was flown at a preselected Mach number. The passing airplane was flown through this flow field at a constant passing rate, and variations in static pressure were measured by a sensitive pressure transducer mounted on the nose boom of the passing airplane. To determine the lateral-separation distance, a motion-picture camera was mounted on the passing airplane to photograph the lead airplane.

Data were obtained on the F-100 and F-104 airplanes at a Mach number of 1.2 and on the B-58 airplane at Mach numbers from 1.3 to 1.8. Lateral-separation distances were from 120 to 425 feet.

RESULTS AND DISCUSSION

A simplified illustration of a supersonic flow field is given in figure 3. The effects of airplane configuration, separation distance, and Mach number on this flow field can be seen by examining figures 4 to 6. Because of the experimental procedure used, the absolute lengths of the flow fields were not determined; therefore, the measured pressures shown in these figures are presented in terms of nondimensional distance between the front and rear shocks.

The effect of airplane configuration can best be seen from figures 4(a) and 5(a), since data for both figures were obtained at a Mach number of 1.2 and a separation distance of 160 feet. The fineness ratios of the two airplanes are approximately the same and it can be seen that the peak bow-wave pressures are also approximately equal. Configuration differences are reflected in the location and strength of the shocks following the bow shock.

The effects of separation distance are apparent in figures 4(a), (b), and (c) and in figures 5(a) and (b). When the separation distance is increased, the shocks decrease in strength and move outward until, eventually, all the shocks have joined with the bow and rear shocks to form an N-shaped wave. This gradual formation of the N-wave is especially evident in figures 4(a), (b), and (c); in figure 4(c), all shocks except one intermediate shock have joined with the bow and rear shocks.

Increasing the Mach number from 1.3 to 1.8 (figs. 6(a), (b), and (c)) has little effect on the flow field. Theoretically, the bow shock-wave pressure increases slightly with increasing Mach number; however, at these Mach numbers and separation distances this is not obvious, since the differences in bow-wave pressures shown in these figures are approximately those predicted for such differences in lateral separation.

To calculate the flow-field pressures, the airplane was replaced by its Mach 1 equivalent body of revolution using the normal cross-sectional-area distribution. The area distributions for the airplanes are shown in figures 7(a), (b), and (c). The flow field was then calculated for this equivalent body by using Whitham's method as outlined in the appendix. This calculated flow field is shown in figures 4 to 6 by the solid lines.

Examination of figures 4 to 6 shows that the bow-wave pressure is predicted fairly well for all three airplanes. However, agreement is better for the F-104 and B-58 than for the F-100, possibly because the F-100 has an open nose and the effective equivalent body of revolution is not estimated as well. The general trends of the flow field are seen in the calculations; however, the additional shocks that originate from airplane components such as the canopy and wings are not accurately predicted either in magnitude or location. In particular, the B-58 flow-field calculation (figs. 6(a) to 6(c)) shows a large negative peak in pressure ratio near the back of the flow field, whereas the experimental data show the negative peak nearly in the center of the flow field.

A possible explanation for this discrepancy in the B-58 flow field is the unusually large percentage of cross-sectional area away from the airplane centerline, since four nacelles are mounted on the B-58 wing. For the F-100 and F-104 airplanes, however, the cross-sectional area is more nearly centered on the airplane axis. Also, the Mach numbers at

which the B-58 was flown were further from the Mach 1 assumption made in determining the equivalent body of revolution.

Another calculation of the B-58 flow field was made, therefore, by using an equivalent body of revolution based on the area intercepted by a series of parallel planes swept at the Mach angle and perpendicular to the longitudinal plane, as shown in figure 7(c) compared with the normal distribution. The results of this flow-field calculation gave much better agreement (fig. 8) with empirical data than was obtained by the previous method. This concept was also used in reference 7 for calculating the wing-body drag at supersonic speeds. This slant cross-sectional area was obtained experimentally by immersing a model in water and measuring the volume displaced. These measurements were taken every 0.2 inch, which corresponds to a body length of $y/l = 0.0114$. Special attention was given to the problem of eliminating any errors caused by the surface tension of the liquid. Previous work had indicated that when a small model is used these errors are significant if the incremental volume displacement is measured by any method requiring liquid flow. To eliminate this possible source of error, displacement rods were used which were extracted slowly as the model was immersed, thereby keeping the liquid level constant. When the results of these measurements were plotted, the maximum scatter was 7 percent of the maximum cross-sectional area.

CONCLUSIONS

The results of flight measurements and calculations of supersonic flow fields indicate that:

1. The strength of the bow shock wave and the overall characteristics of the flow field can be estimated fairly well by using simple theory; however, the location and magnitudes of all the intermediate shocks are not accurately predicted.

2. The normal-area distribution used in the theory may not be an adequate representation of an equivalent body of revolution for estimating the entire flow field, especially at Mach numbers much greater than 1. Using an equivalent body of revolution based on the area intercepted by parallel planes swept at the Mach angle greatly improved the results of the calculations.

Flight Research Center,
National Aeronautics and Space Administration,
Edwards, Calif., August 22, 1960.

APPENDIX

PROCEDURE USED FOR CALCULATING FLOW FIELD

The theory developed by Whitham is given in detail in reference 3. A numerical solution of the $F(y)$ integral appearing in the theory is given in this appendix, along with a brief summary of the method used to calculate the flow field.

From reference 3

$$\frac{\Delta p}{p_0} = \frac{\gamma M^2}{\sqrt{2\beta}} \frac{F(y)}{r^{1/2}} \tag{1}$$

$$x = \beta r - kF(y)r^{1/2} + y \tag{2}$$

Where

$$k = 2^{-1/2}(\gamma + 1)M^4\beta^{-3/2}$$

and $F(y)$ is a function determined by the body shape and for a smooth slender body is

$$F(y) = \frac{1}{2\pi} \int_0^y \frac{S''(t)dt}{\sqrt{y - t}} \tag{3}$$

If no analytical expression is known for the area distribution, $F(y)$ must be integrated numerically. Equation (3) is a form of Abel's integral equation and, because of the singularity of the integrand at the upper limit, the transform

$$S'(t) = 2 \int_0^t \frac{F(y)dy}{\sqrt{t - y}} \tag{4}$$

is used to solve numerically for $F(y)$ in the following manner.

Assume $F'(y)$ is a constant over a small interval Δy. Then $F(y)$ can be written

$$F(y) = F(y)_i + F'(y)_{i+1}\left(y - y_i\right) \tag{5}$$

over the interval

$$y_i \leqq y \leqq y_{i+1}$$

where

$$i = 0, 1, 2, \ldots m$$

and

$$y_0 = F(y)_0 = 0$$

Then

$$\frac{1}{2}S'\left(y_{n+1}\right) = \sum_{i=0}^{n} \int_{y_i}^{y_{i+1}} \frac{\left[F_i + F'_{i+1}\left(y - y_i\right)\right] dy}{\sqrt{y_{n+1} - y}} \tag{6}$$

The integral in equation (6) can easily be integrated to give

$$\frac{1}{2}S'\left(y_{n+1}\right) = \sum_{i=0}^{n} -2\left(F_i - F'_{i+1}y_i\right)\left[\left(y_{n+1} - y_{i+1}\right)^{1/2} - \left(y_{n+1} - y_i\right)^{1/2}\right]$$

$$+ 2F'_{i+1}\left[\frac{\left(y_{n+1} - y_{i+1}\right)^{3/2}}{3} - y_{n+1}\left(y_{n+1} - y_{i+1}\right)^{1/2}\right.$$

$$\left. - \frac{\left(y_{n+1} - y_i\right)^{3/2}}{3} + y_{n+1}\left(y_{n+1} - y_i\right)^{1/2}\right] \tag{7}$$

The only unknown in equation (7) is F'_{n+1}. When this is found, the next value for $F(y)$ is known. By this step process the entire $F(y)$-curve can be constructed.

Once the $F(y)$-curve is known, it is then simple to find the shocks. Whenever $F'(y) > 0$ a shock will appear. To find the bow shock, an integrator can be used and, by trial and error, values of y and $F(y)$ can be found for which

$$\frac{1}{2}kr^{1/2}F^2(y) = \int_0^y F(t)dt \tag{8}$$

These values are then used in equations (1) and (2) to determine the position and strength of the bow shock.

To find the other shocks, lines with slopes which are given by

$$\frac{F(y_2) - F(y_1)}{y_2 - y_1} = \frac{1}{kr^{1/2}} \tag{9}$$

are drawn through the $F(y)$-curve such that "lobes" cut off on each side of the curve are equal in area (see following sketch). These, then, are the values of $F(y)$ and y to be used in equations (1) and (2).

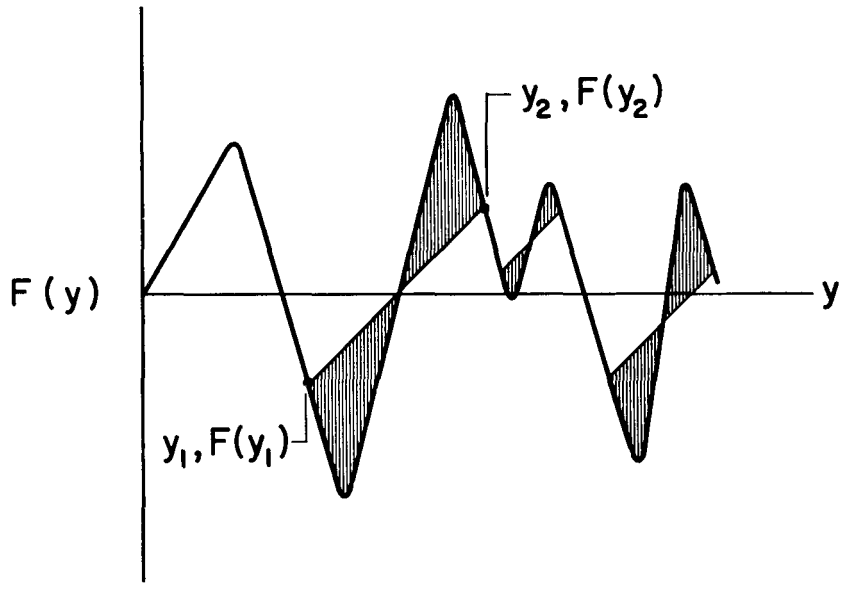

REFERENCES

1. Jordan, Gareth H.: Some Aspects of Shock-Wave Generation by Supersonic Airplanes. AGARD Rep. 251, North Atlantic Treaty Organization, Sept. 1959.

2. Ferri, Antonio: Application of the Method of Characteristics to Supersonic Rotational Flow. NACA Rep. 841, 1946.

3. Whitham, G. B.: The Flow Pattern of a Supersonic Projectile. Communications on Pure and Appl. Math., vol. V, no. 3, Aug. 1952, pp. 301-348.

4. Mullens, Marshall E.: A Flight Test Investigation of the Sonic Boom. AFFTC TN-56-20, May 1956.

5. Daum, Fred L., and Smith, Norman: Experimental Investigation of the Shock Wave Pressure Characteristics Related to the Sonic Boom. WADC TN-55-203, Aug. 1955.

6. Carlson, Harry W.: An Investigation of Some Aspects of the Sonic Boom by Means of Wind-Tunnel Measurements of Pressures About Several Bodies at a Mach Number of 2.01. NASA TN D-161, 1959.

7. Jones, Robert T.: Theory of Wing-Body Drag at Supersonic Speeds. NACA Rep. 1284, 1956.

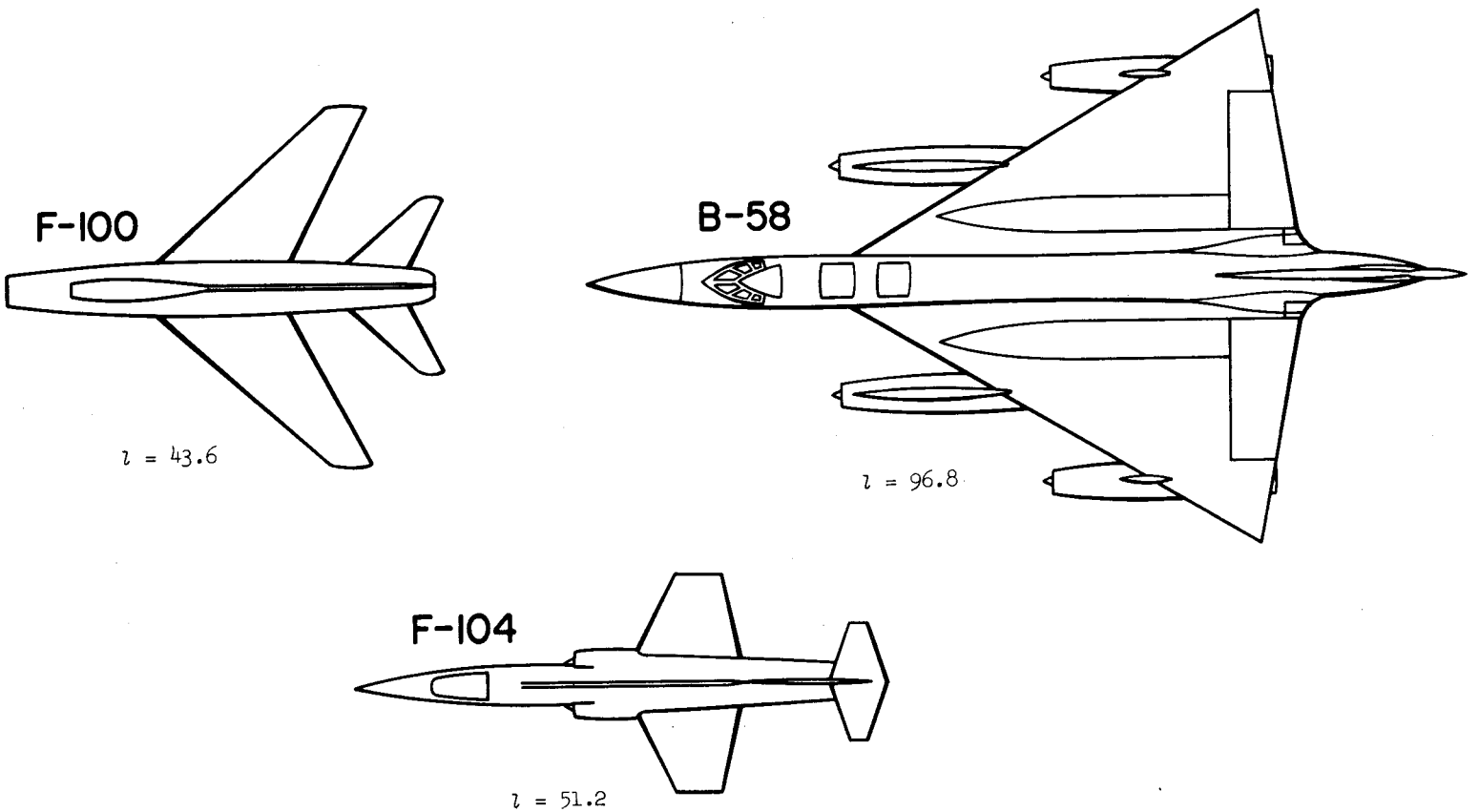

Figure 1.- Plan views of the airplanes showing relative sizes. Dimensions are in feet.

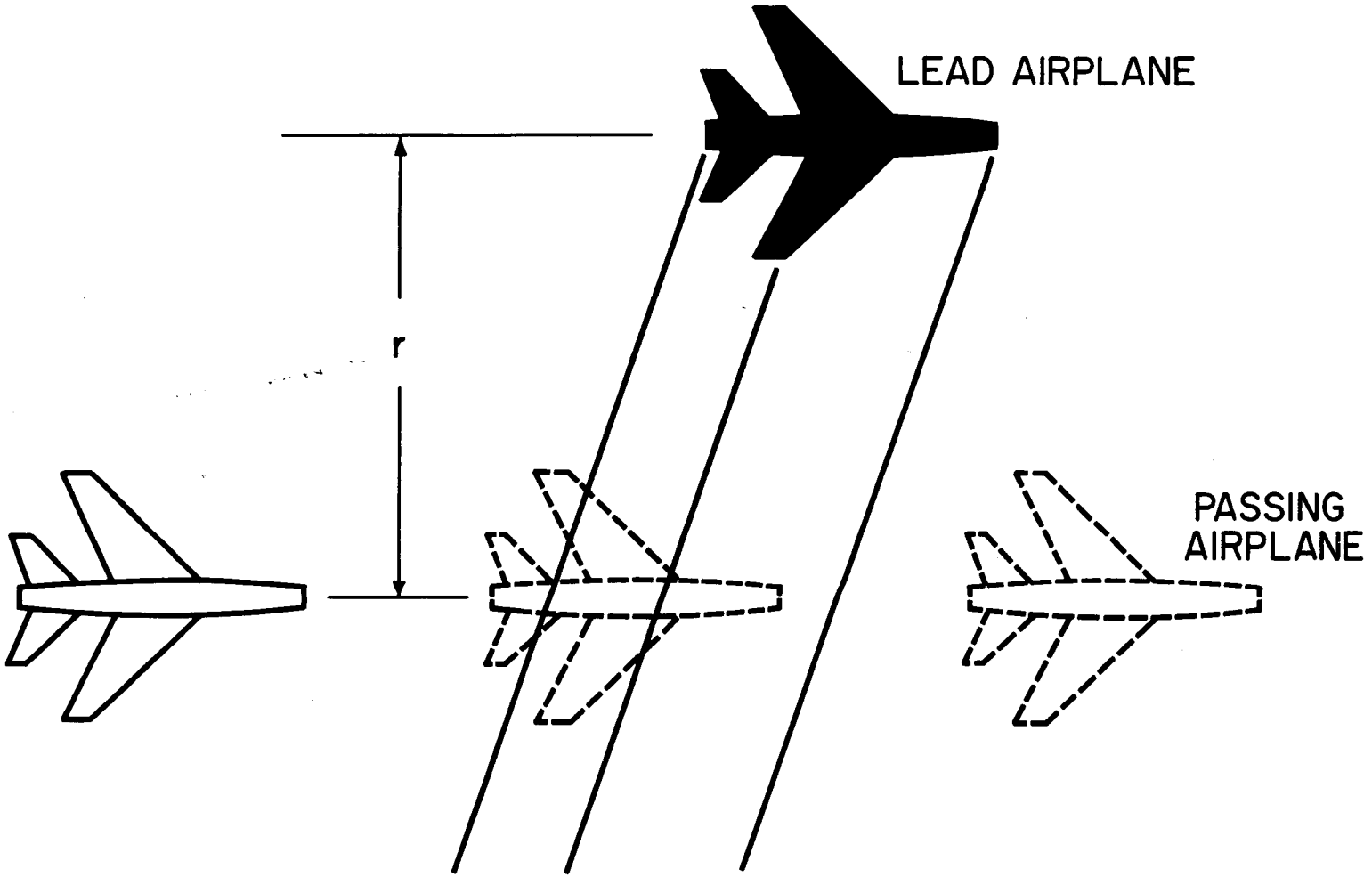

Figure 2.- Illustration of tests.

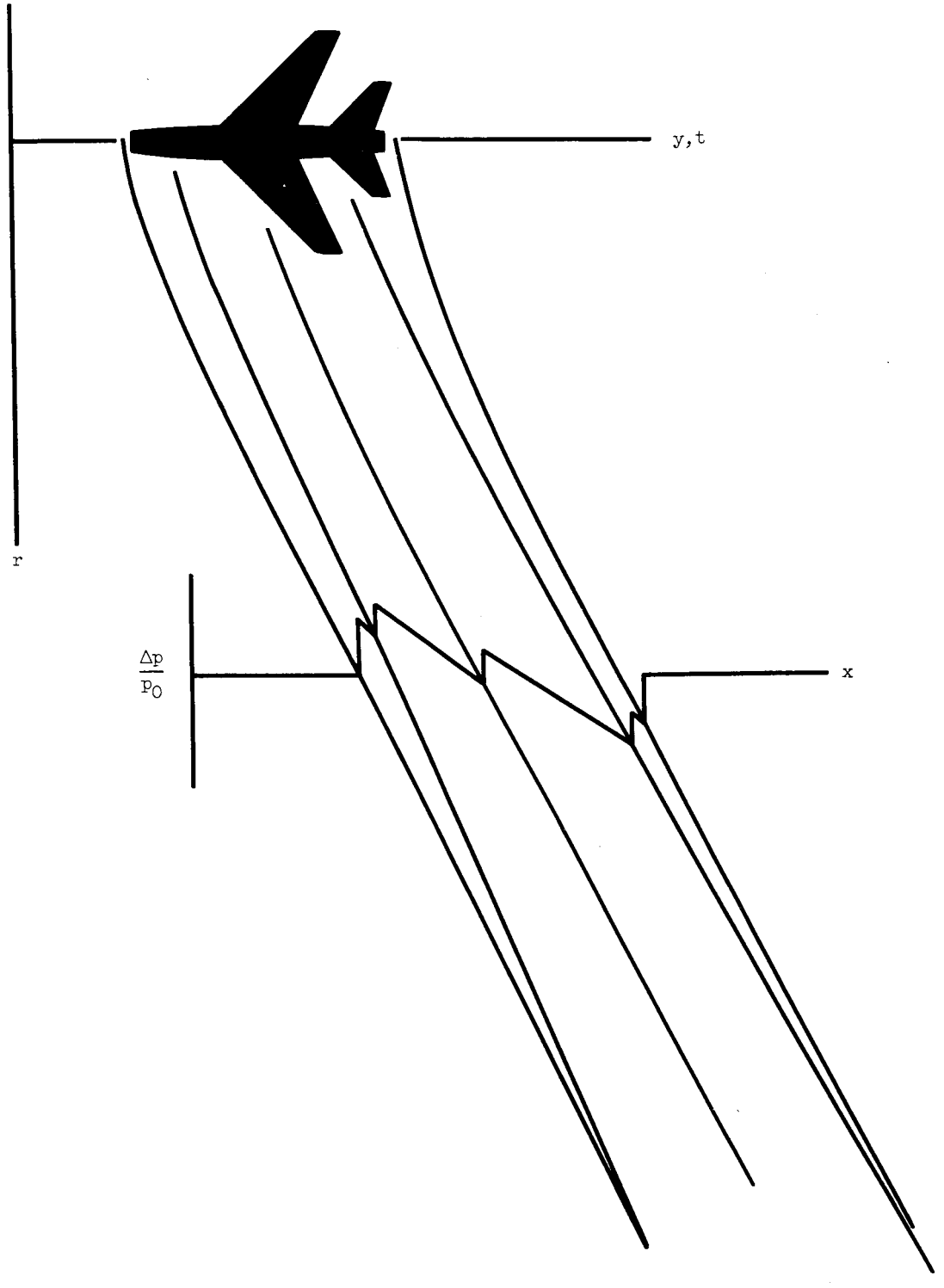

Figure 3.- Sketch of supersonic flow field.

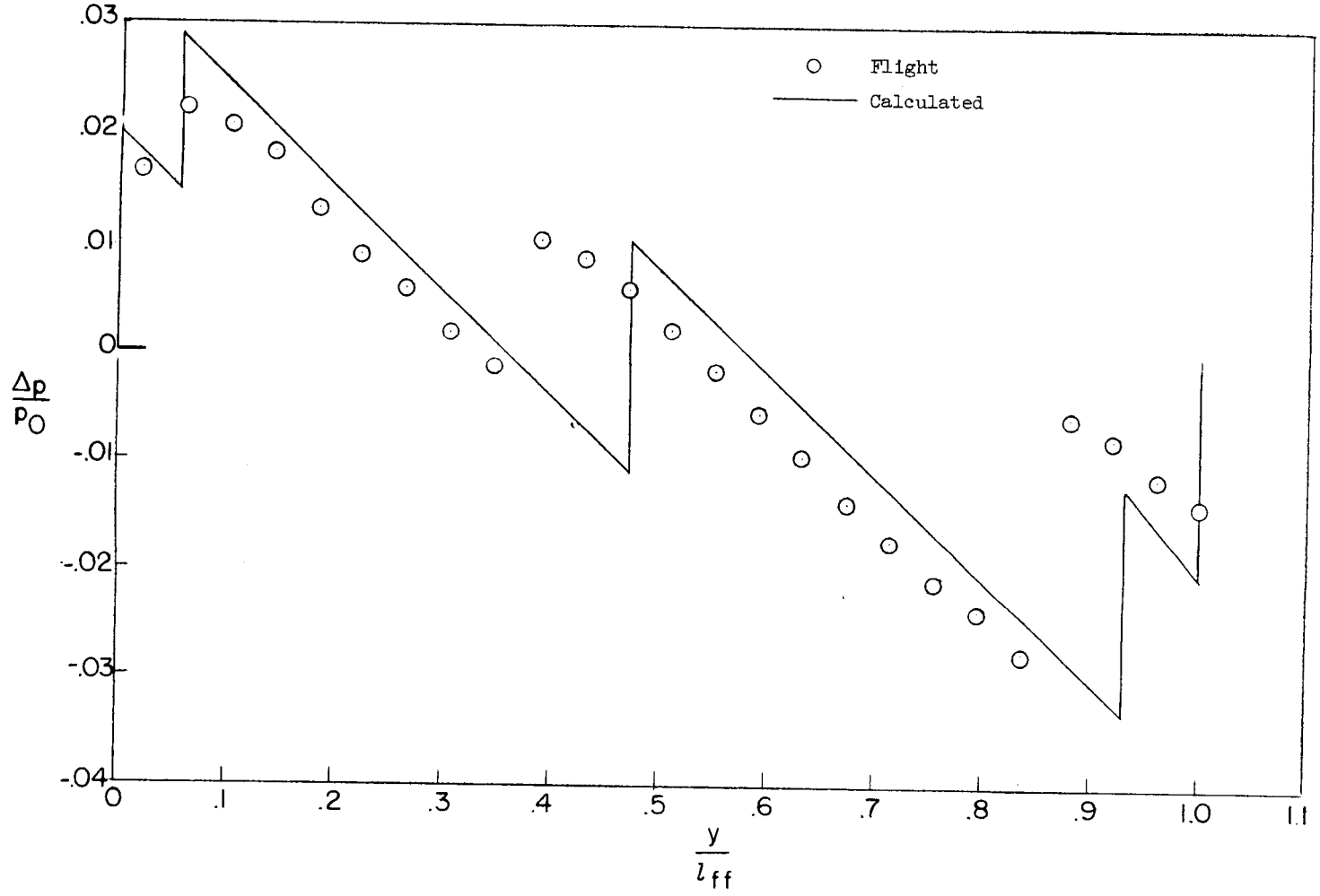

(a) r = 160 feet.

Figure 4.- F-100 flow field. M = 1.2.

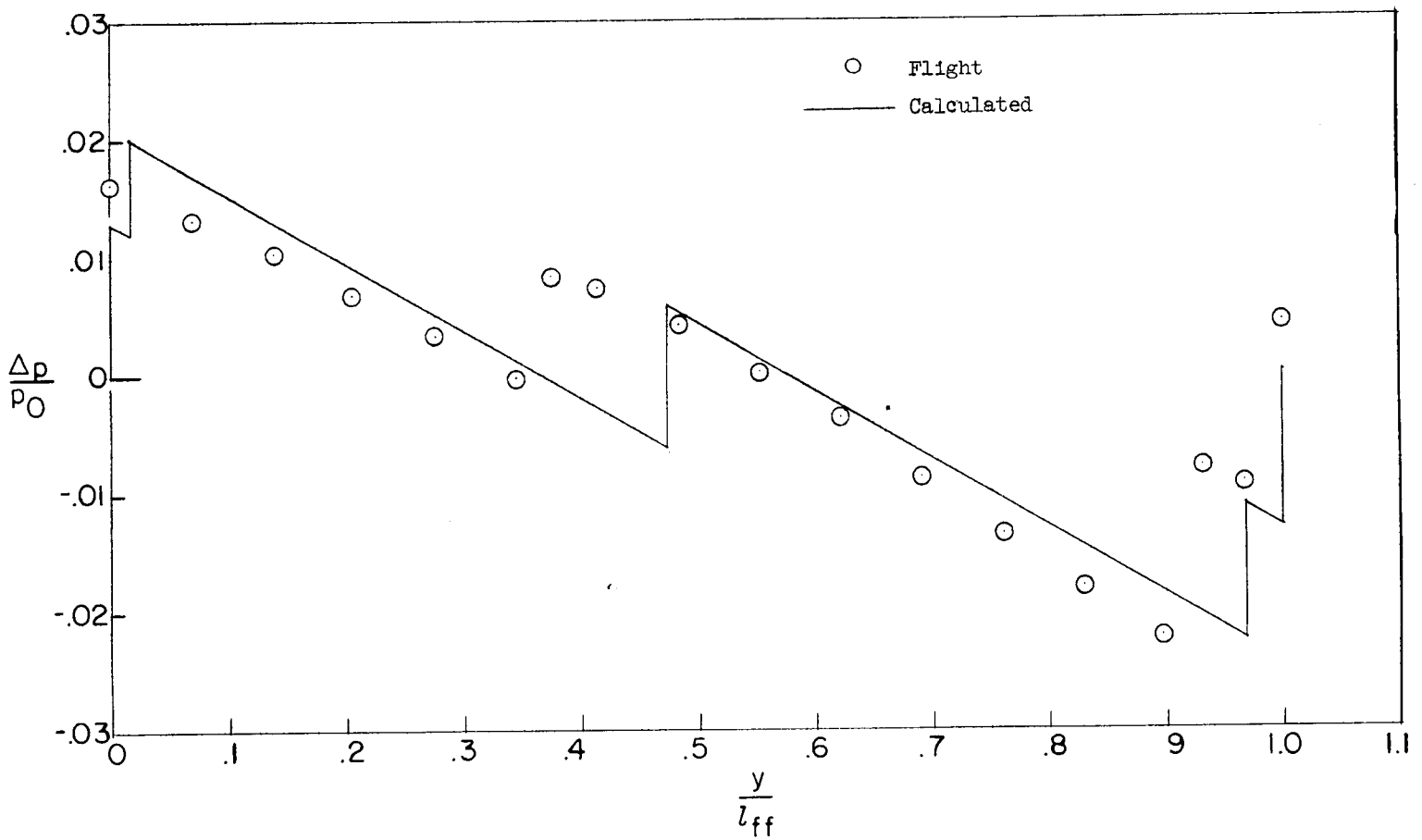

(b) r = 290 feet.

Figure 4.- Continued.

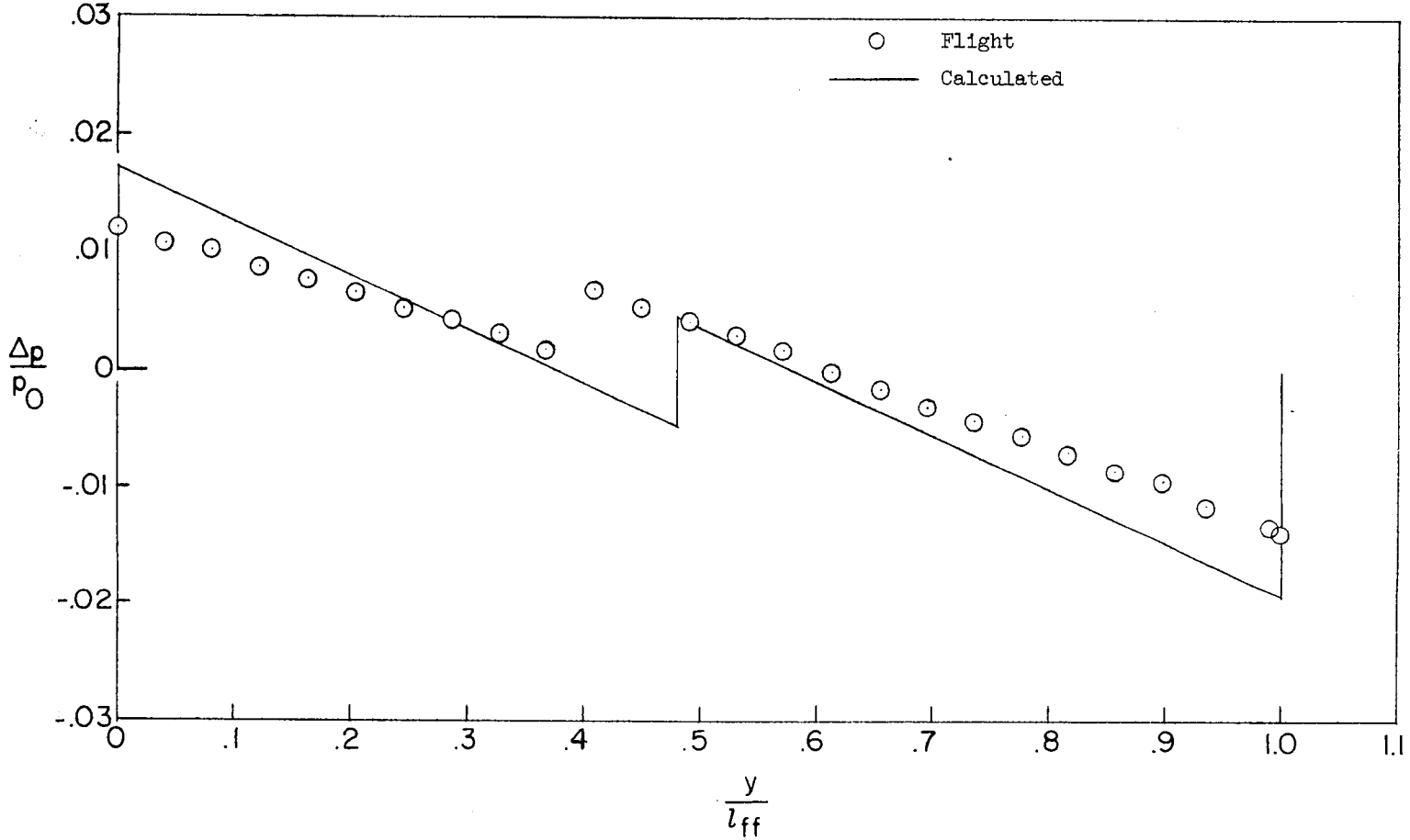

(c) r = 370 feet.

Figure 4.- Concluded.

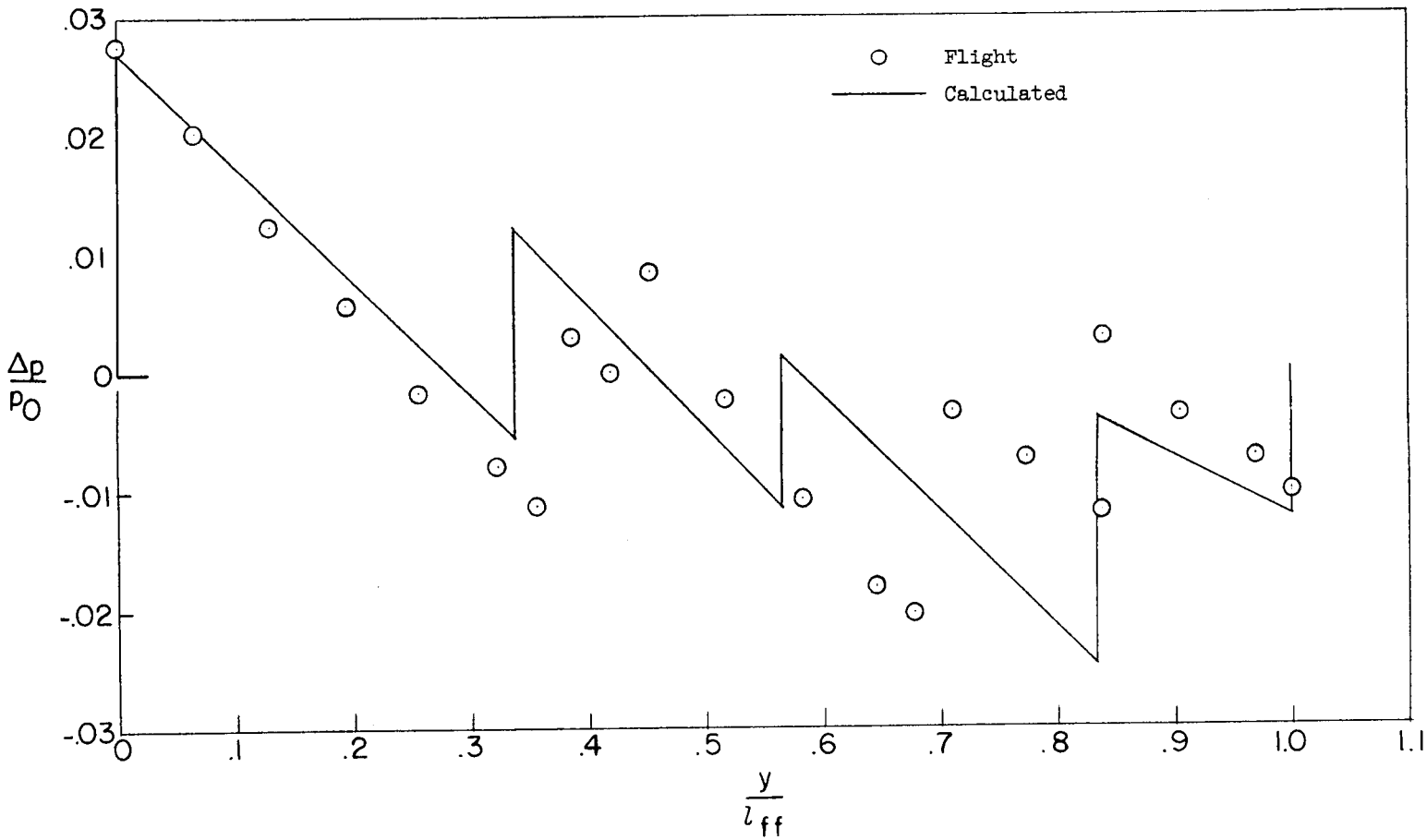

(a) r = 160 feet.

Figure 5.- F-104 flow field. M = 1.2.

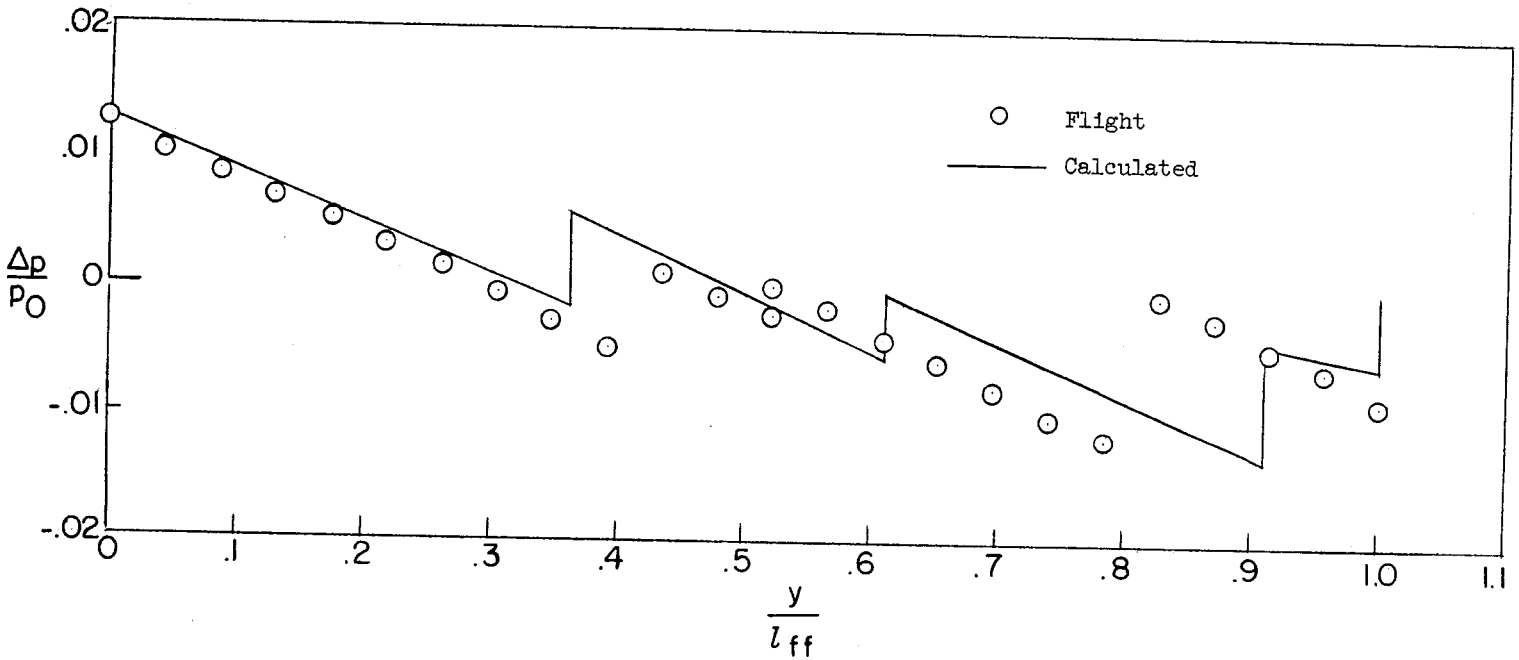

(b) r = 425 feet.

Figure 5.- Concluded.

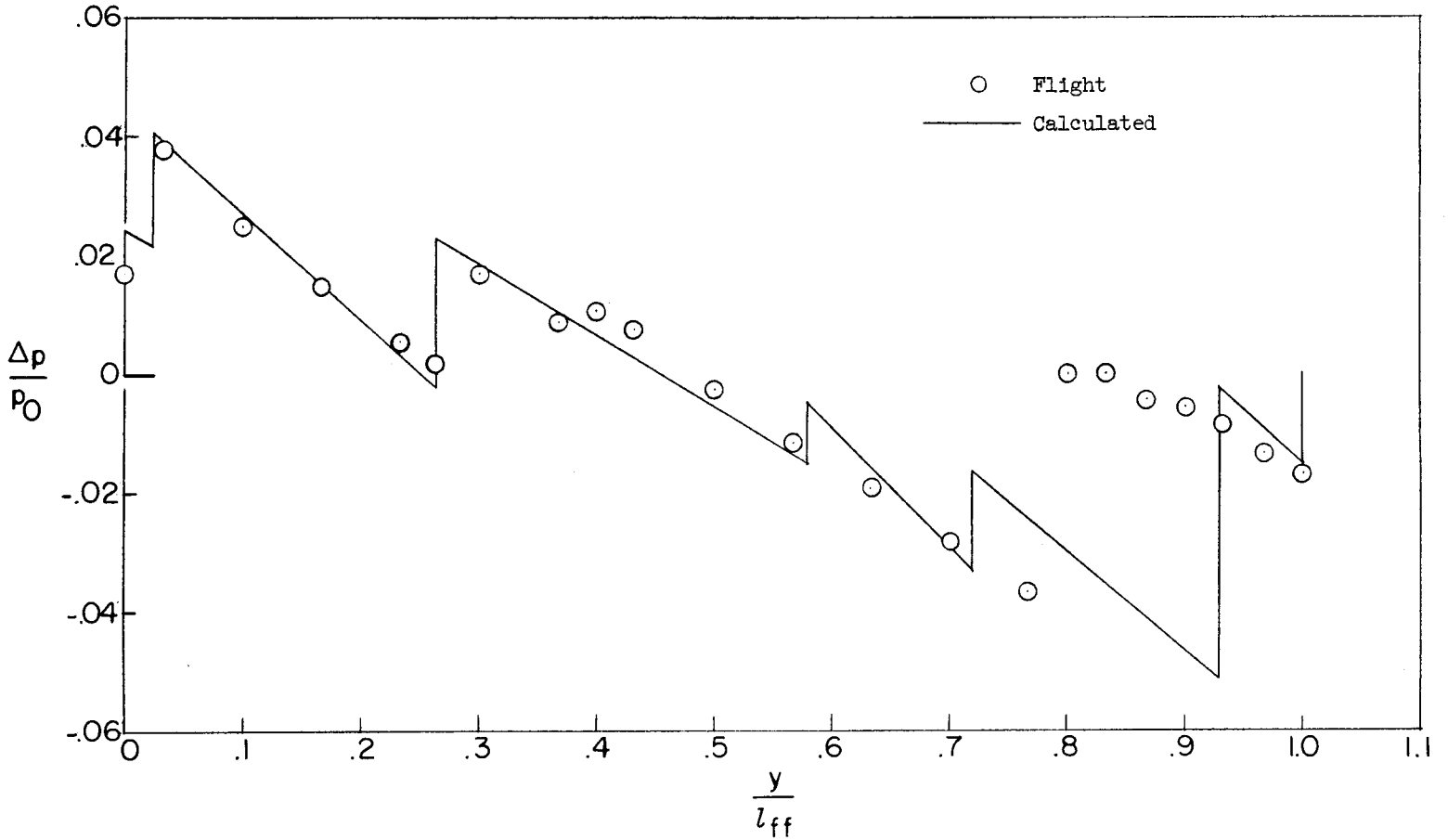

(a) M = 1.3, r = 150 feet.

Figure 6.- B-58 flow field.

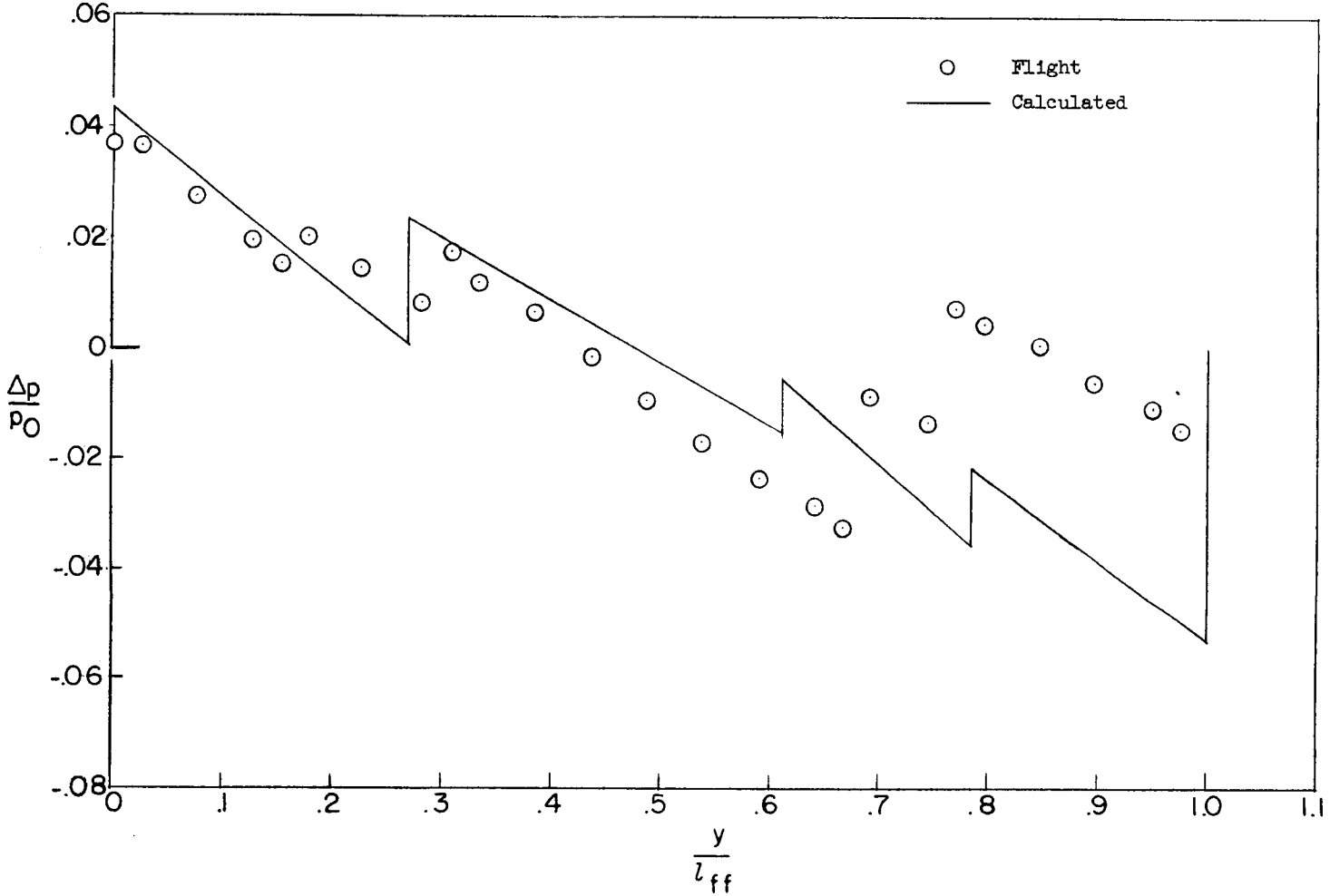

(b) M = 1.6, r = 180 feet.

Figure 6.- Continued.

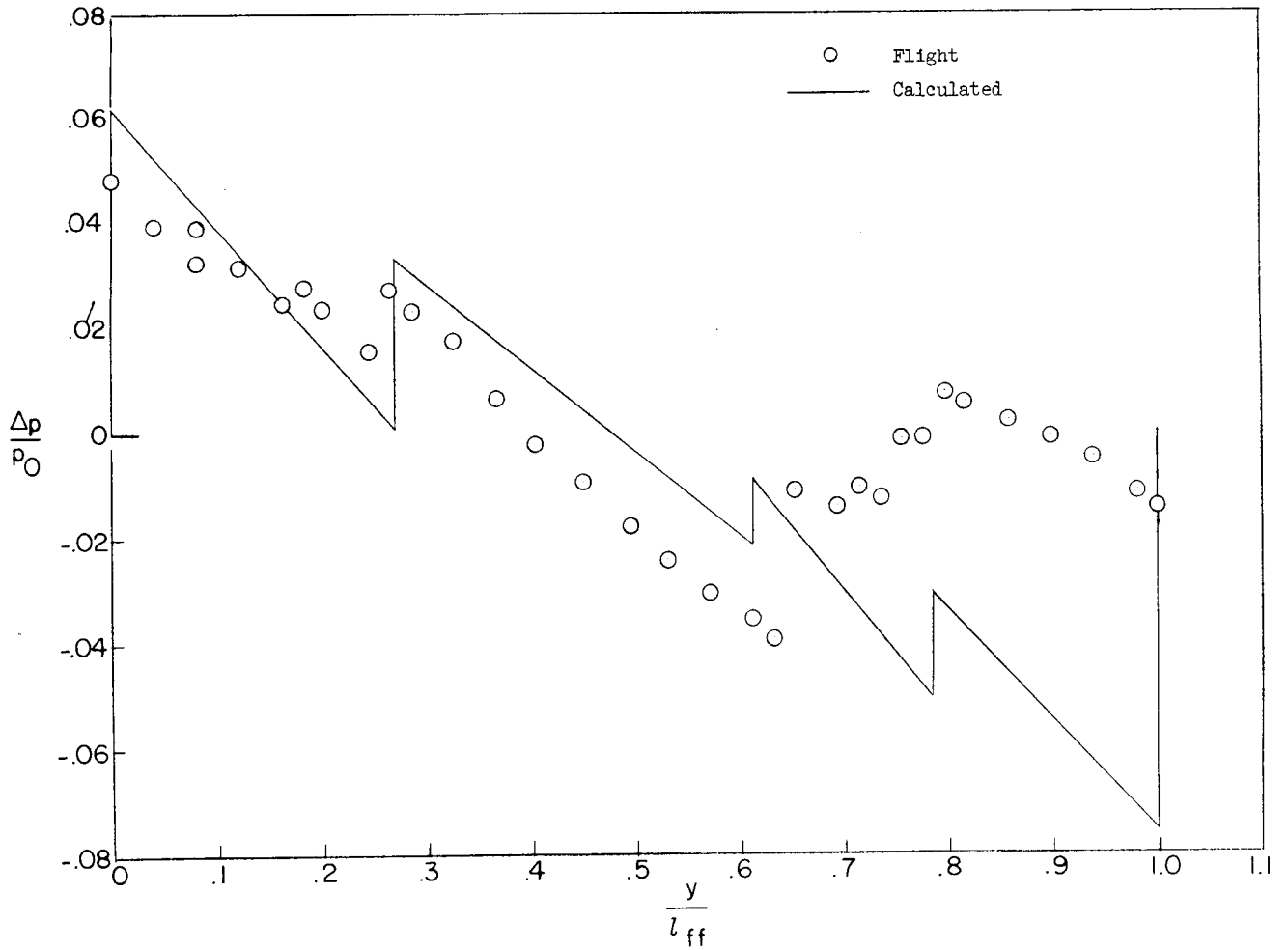

(c) M = 1.8, r = 120 feet.

Figure 6.- Concluded.

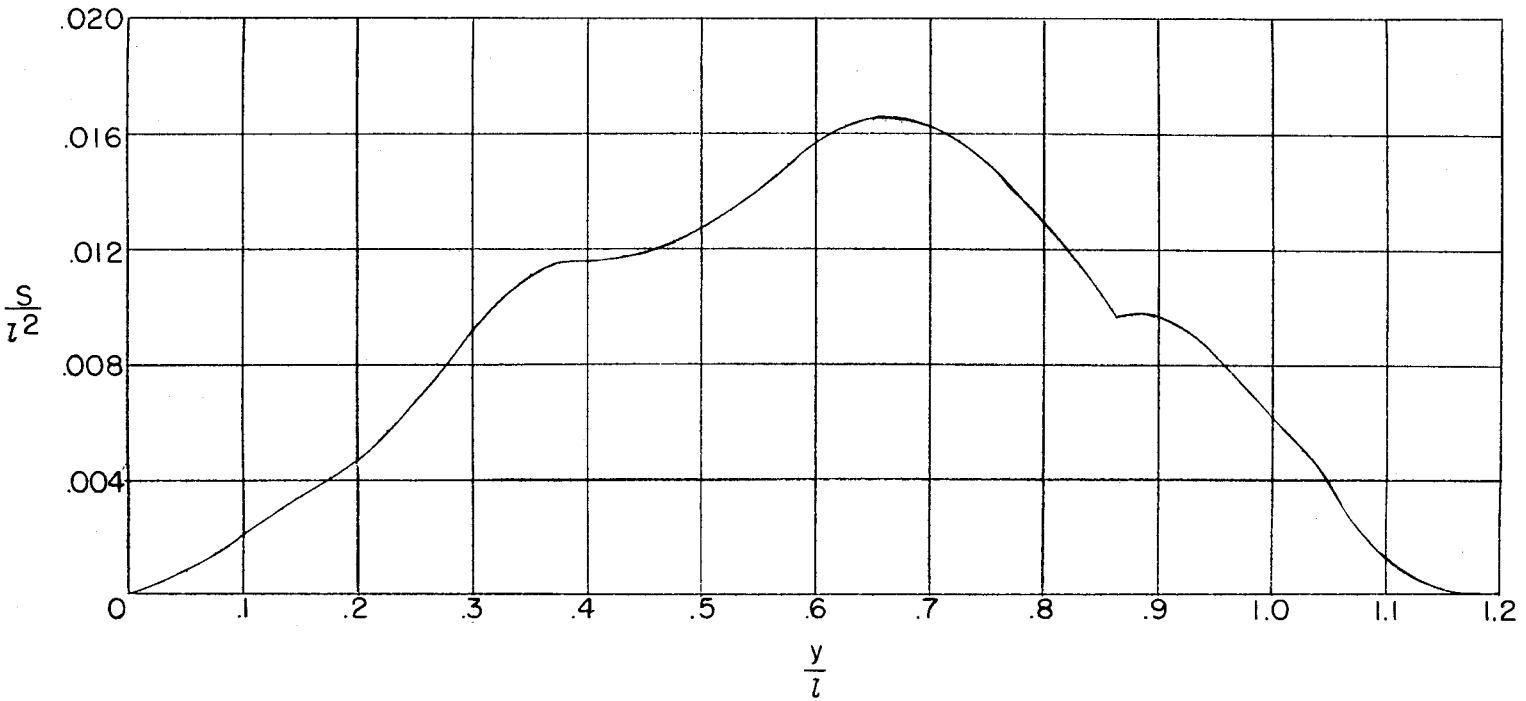

(a) F-100.

Figure 7.- Area distribution.

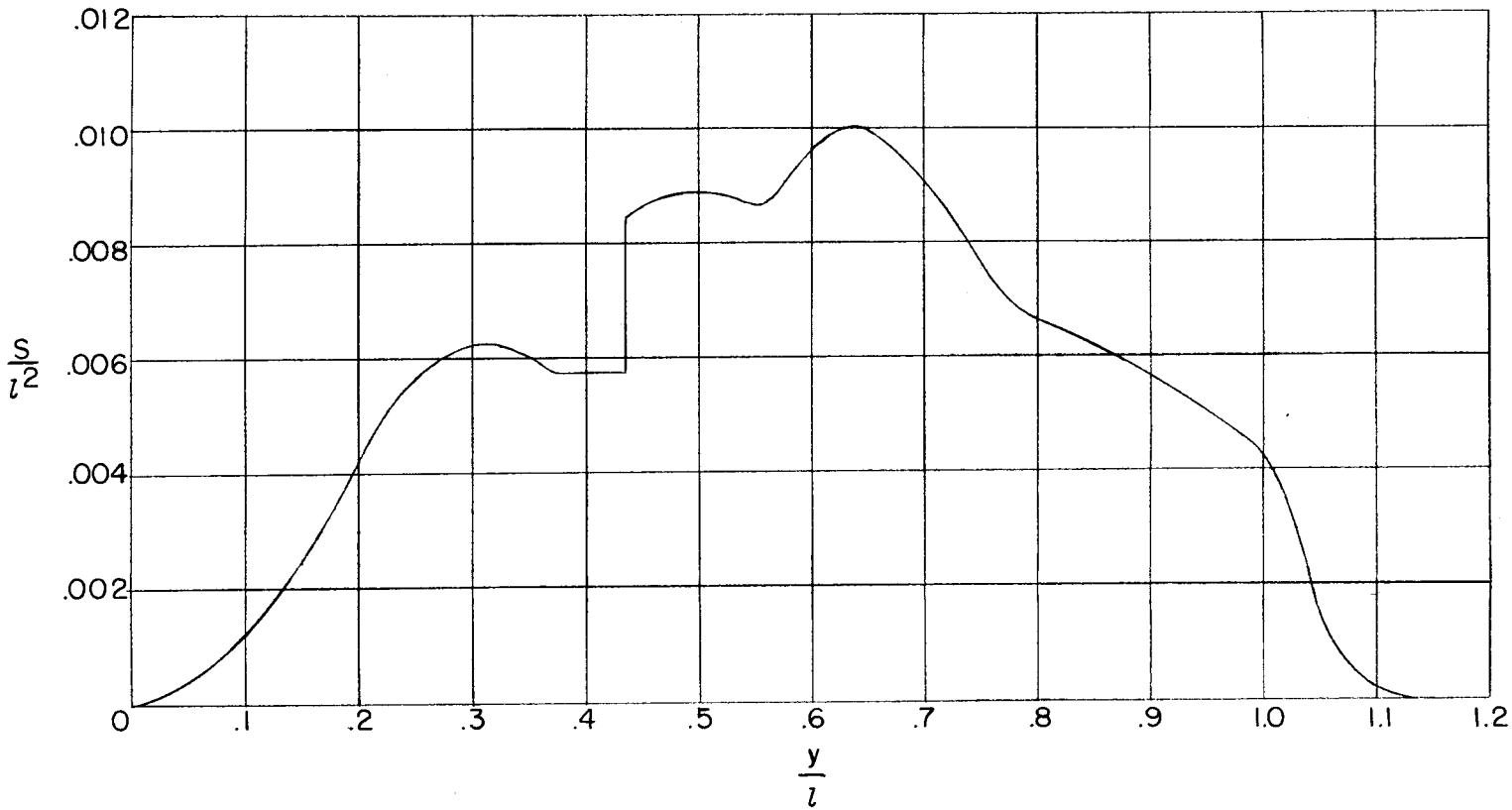

(b) F-104.

Figure 7.- Continued.

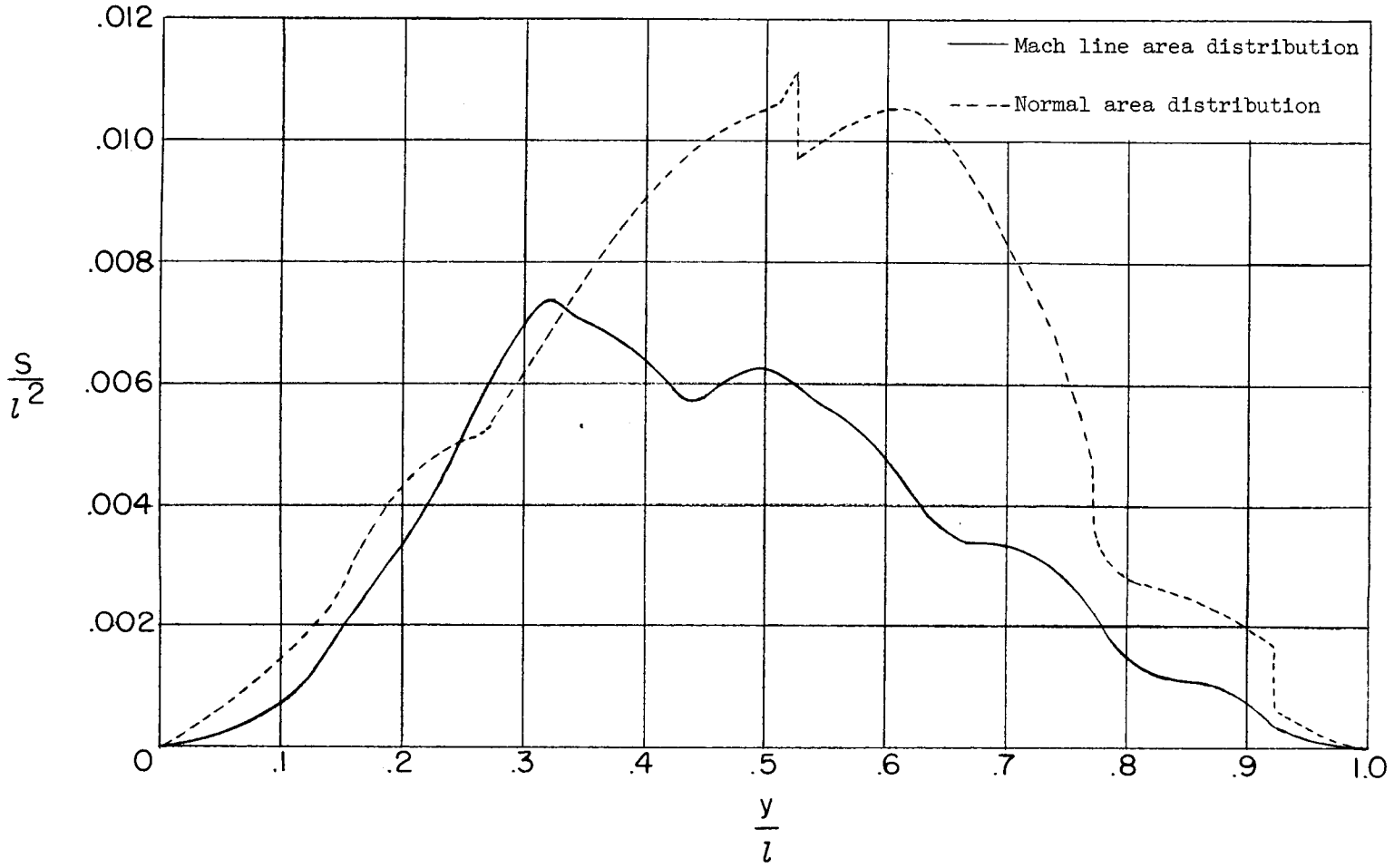

(c) B-58.

Figure 7.- Concluded.

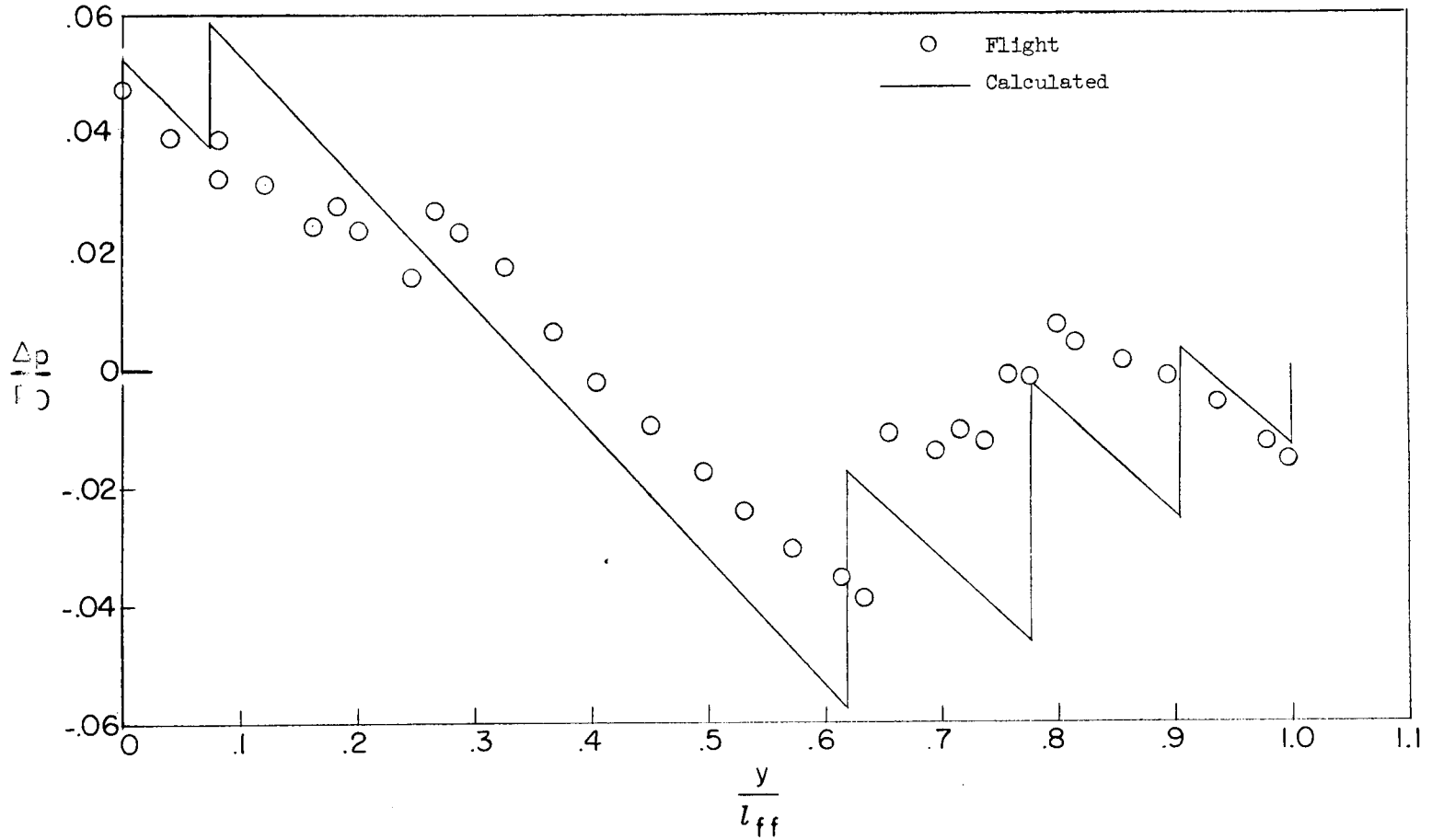

Figure 8.- Calculated curve of B-58 flow field based on Mach line area distribution. M = 1.8; r = 120 feet.